

SCIENTIFIC REPORTS

Corrected: Retraction

OPEN

Inhibition of airway inflammation in a cockroach allergen model of asthma by agonists of miRNA-33b

Ruichao Niu¹, Xuping Xiao², Bin Liu², Yunqiu Li², Yuzhong Yu² & Lijuan Ma²

MicroRNAs (miRNAs) play powerful roles in immune function by regulating target genes that mediate cell behavior. It is well known that mast cells have essential effector and immune regulatory functions in IgE-associated allergic disorders and in innate and adaptive immune responses. However, the role of miRNAs in mediating mast cell functions and the relevant mechanisms require further exploration. The roles of miR-33b in airway inflammation and mast cell functions are still unknown. To examine the role of miR-33b in mouse mast cells in cockroach allergen-induced asthma, we developed a lentiviral system for miRNA-33b overexpression to examine whether miRNA-33b mediates airway inflammation by regulating mast cell function and to evaluate the underlying mechanism. The results showed that miR-33b inhibited cockroach allergen-induced asthma *in vivo*: in particular, it inhibited T_H2 cytokine production. In addition, we found that in cells in which miRNA-33b had been transfected, mast cell degranulation was inhibited through suppression of the calcium release and IgE/FcεRI pathway. Our study provides new insight into the roles of miR-33b in asthma and mast cell biology and identifies novel mechanisms that may contribute to mast cell-related pathological conditions in airway inflammation.

Asthma is characterized by airway obstruction and inflammation, mucus overproduction, airway hyper-responsiveness (AHR) and high IgE production in response to environmental factors and allergy¹. Allergic inflammation is a response to activation of the Th2 pathway involving the production of IL-4, IL-5, and IL-13². Exposure to specific allergens, such as ovalbumin (OVA), house dust mite allergen (HDM), cockroach allergen (CRE), or non-specific triggers such as air pollution can induce the airway inflammation that occurs during asthma. Exposure to CRE has been linked to severe respiratory symptoms. In fact, sensitization to CRE has been identified as one of the strongest risk factors for the development of asthma⁵. Mast cells are known to play a critical role in the regulation of allergic responses. Mast cells can be activated by numerous cytokines and inflammatory mediators and can contribute to various pathophysiological events in acute and chronic inflammation^{6,7}. The classical activation of mast cell-specific signaling is initiated through antigen- and IgE-dependent aggregation of the high affinity IgE receptor, FcεRI, which is present on surfaces of mast cells. Events downstream of the early FcεRI-induced signaling event (such as Ca²⁺ influx) are crucial processes in mast cell degranulation⁷.

miRNAs are small non-coding RNAs that post-transcriptionally regulate gene expression by targeting the 3'-untranslated region of specific messenger RNAs (mRNAs)⁸. Evidence has recently suggested that miRNAs play a critical role in the development of asthma^{9,10}. Furthermore, mast cell activation can be regulated by several of miRNAs. MiR-221 and miR-222 significantly increase the degranulation and adherence of mast cells^{11,12}. MiR-126 has been shown to positively regulate mast cell proliferation by targeting the negative regulator of mast cell proliferation Spred1¹³. Another study showed that miR-132 was the most important miRNA in the activation of mast cell degranulation¹⁴. It is known that miR-33b is encoded within intron 17 of the Srebp-1 gene on chromosome 17¹⁵. MiR-33b has been reported to inhibit cancer development by regulating the cell cycle¹⁶⁻¹⁹. Takwi found that lovastatin up-regulates miR-33b expression, reduces cell proliferation and impairs c-Myc expression in medulloblastoma cells²⁰. However, no study has described miR-33b expression in airway inflammation or in mast cells. We therefore hypothesized that miR-33b can inhibit CRE-induced asthma by controlling mast cell activation.

¹Department of Respiratory Medicine, Xiangya Hospital, Central South University, Changsha, 410008, P.R. China.

²Department of Otolaryngology Head and Neck Surgery, Hunan Provincial People's Hospital, The First Affiliated Hospital of Hunan Normal University, Changsha, 410008, P.R. China. Correspondence and requests for materials should be addressed to L.M. (email: lijuanma0925@163.com)

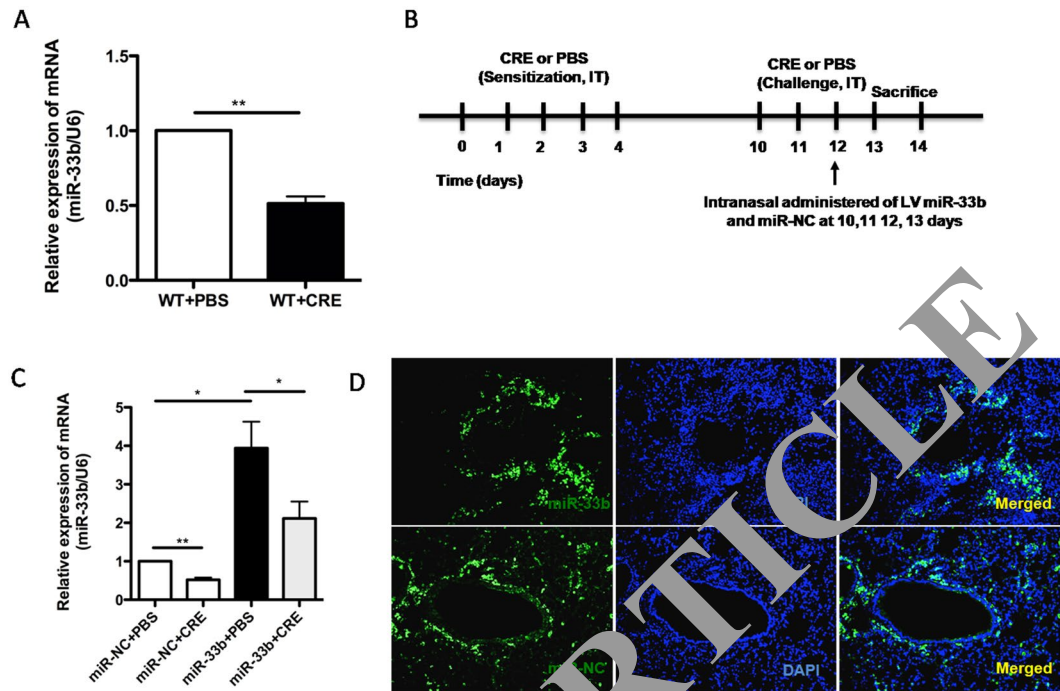


Figure 1. Expression of lentiviral miR-33b in the asthmatic mice. **(A)** qRT-PCR was used to evaluate miR-33b expression in CRE-challenged WT mice. **(B)** C57BL/6 mice were sensitized on days 0 and 4 with intra-tracheal instillations of 400 $\mu\text{g}/\text{ml}$ CRE. Non-sensitized control animals received the same volume of PBS alone. Five days after the first sensitization, the mice were challenged intra-tracheal instillation of the same concentration of CRE once only on days 10 and 13. In addition, during the challenge period, the mice were intra-nasally administered 2×10^6 infectious units (IFUs) of LV miR-33b or 2×10^6 IFUs of an empty LV vector. **(C)** qRT-PCR was used to test miR-33b expression in the miR-33b or miR-NC transfected model. **(D)** Representative images of GFP immunofluorescence in lung tissue sections of CRE-challenged WT mice that were transfected with miR-NC or miR-33b ($n = 4$). The data are representative of three independent experiments ($n = 4$ –6 mice/group). The data are presented as mean \pm SEM. * $P < 0.05$, ** $P < 0.01$.

The present study was the first to examine the role of miR-33b in the inhibition of CRE allergen-induced asthma and to quantify miR-33b expression in IgE-mediated suppression of mast cell function. In addition, the potential mechanistic pathway was investigated.

Methods

All methods were performed in accordance with the relevant guidelines and regulations of the Central Laboratory at Hunan Provincial People's Hospital.

Mice. All mice were maintained under specific pathogen-free conditions. The experiments were performed with gender-matched mice aged 6–8 weeks. The Animal Care and Use Committee at Hunan Provincial People's Hospital approved all protocols. The mice were sensitized on days 0 to 4 with an intra-tracheal instillation of 400 $\mu\text{g}/\text{ml}$ of a whole-body extract of German cockroaches (CRE, *Blattella germanica*). Non-sensitized control animals received the same volumes of PBS alone. Five days after the first sensitization, the mice were challenged with a single intra-tracheal instillation of the same concentration of CRE on days 10 to 13. In addition, during the challenge period, the mice were intra-nasally administered 2×10^6 infectious units (IFUs) of lentiviral miR-33b or 2×10^6 IFUs of an empty lentiviral vector. For *in vivo* engraftment, C57BL/6 mice were intravenously injected with *in vitro*-generated BMMCs that had been transfected with miR-33b or miR-NC at 9 days (1×10^7 per mouse). The C57BL/6 mice then were challenged with CRE as described before. MiR-33b was generated by lentiviral transduction, and the transduction was carried out according to advice from GENECHEM¹⁷.

qRT-PCR. The miR-33b primer was prepared according to our previously published paper¹⁷. U6 was selected as the endogenous control for miR-33b. The relative quantification of target gene expression was evaluated using the $2^{-\Delta\Delta\text{CT}}$ method. The miR-33b (HmiRQP0432) and U6 (HmiRQP9001) primers were purchased from Genecopia¹⁷.

Lung histology. The lungs were fixed in 4% formaldehyde, and 5 μm sections were stained with hematoxylin and eosin (HE) or with periodic acid Schiff (PAS) reagent and examined using a Nikon microscope (X10 magnification). The bronchial infiltrates were independently assessed by three observers using a semiquantitative

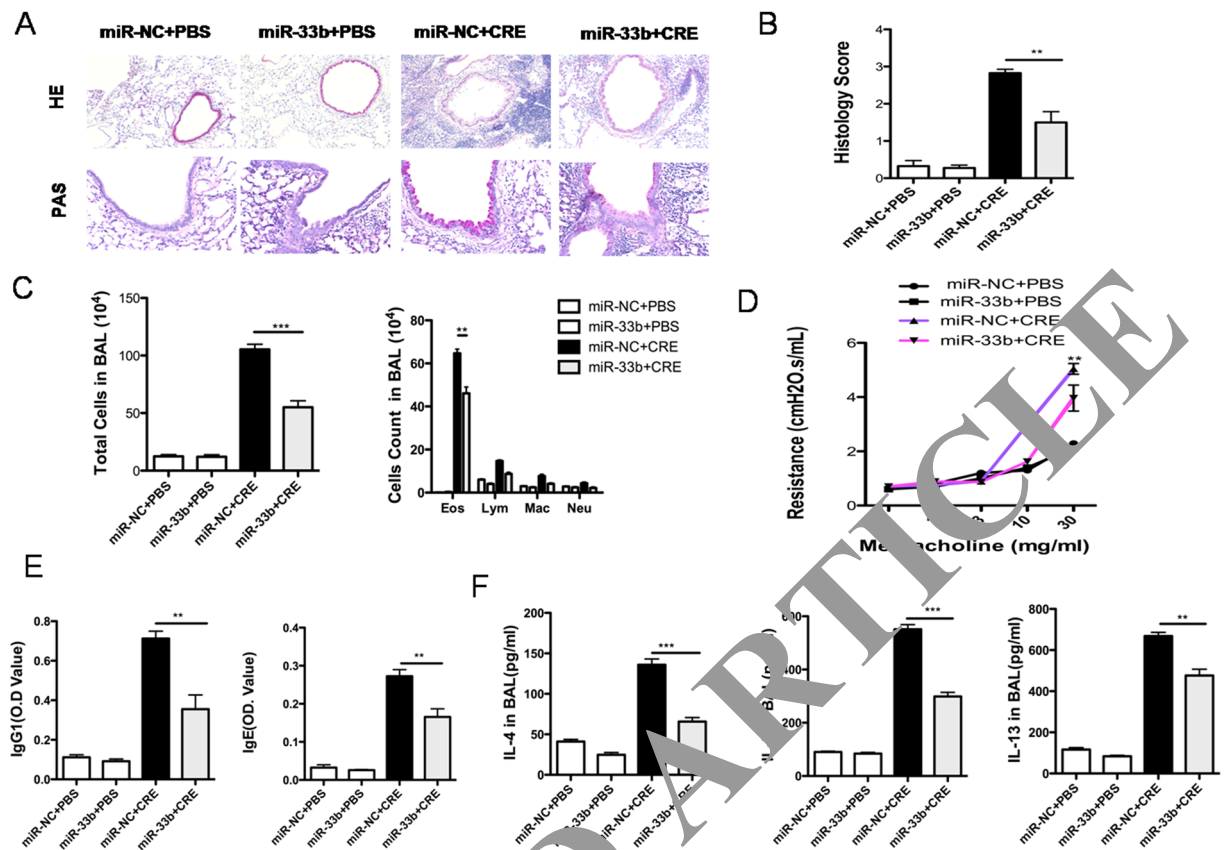


Figure 2. MiR-33b regulates eosinophilic flux and lung inflammation in response to CRE. (A) Inflammation in pulmonary sections of the PBS and CRE groups of mice that were transfected with miR-33b or miR-NC. Representative images of the central airways stained with hematoxylin and eosin (HE) and periodic acid-Schiff (PAS) staining. (B) Histology scores of the HE staining. (C) Cellular inflammation, as reflected by the total cell number and differentiated leukocyte cell numbers in the BALF. (D) Airway hyper-responsiveness to methacholine (Mch) was analyzed in the various groups. (E) Serum levels of cockroach allergen-specific IgE and IgG1 (F) Th2 cytokines IL-4, -5 and -13 in the BALF. The data are representative of three independent experiments ($n = 4-6$ mice/group). The data are presented as the means \pm SEM. ** $P < 0.01$, *** $P < 0.001$.

score (0–21). Images were obtained using a NIKON ECLIPSE Ti-U microscope equipped with a DS-Fi2 camera (NIKON, USA).

Analysis of lung inflammation. IL-4, IL-5, IL-13, IgE and IgG1 in BALF were measured using commercially available enzyme-linked immunosorbent assay (ELISA) kits from eBioscience according to the manufacturer's recommendations. Flow cytometry was used to test the percentages of the various inflammatory cells in the BAL. Eosinophils were defined as SSC^{high} SiglecF⁺ (clone E50-2440, BD) Mac-3⁻ (M3/84, BD) cells, alveolar macrophages were identified as SSC^{high} SiglecF⁺ Mac-3⁺ cells, granulocytes were recognized as SSC^{high} Gr-1⁺ (clone RB6-8C5, eBioscience) cells, and lymphocytes were identified as FSC^{low}/SSC^{low} and expressing CD3 (clone 145-2C11, eBioscience) or CD19 (clone 1D3, eBioscience).

Determination of lung function. For invasive measurements of dynamic resistance, the mice were anesthetized by intraperitoneal injection of a solution containing ketamine and xylazine. Ventilation was initiated with a volume-cycled ventilator (Flexivent; SCIREQ Scientific) with a positive end-expiratory pressure of 2 cmH₂O. Airway responsiveness was measured by challenging the mice with increasing doses of aerosolized methacholine (Mch, 0–30 mg/mL). The pulmonary resistance and compliance were measured with Flexivent software and exported to Pulmodyn data-acquisition software (Hugo Sachs Electronic) for further data analysis.

DAB staining of mast cells. For DAB staining, after antigen retrieval, slides of deparaffinized embedded tissue sections were blocked with 3% BSA containing 0.1% TX100 and 0.1% NaN₃ for 1–2 h at room temperature (RT) with rocking. The primary antibody solution consisted of a 1:200 dilution of the anti-mast cell tryptase antibody ab2378 (Abcam) overnight. On the second day, the slides were treated with a 1:200 dilution of the secondary antibody, goat anti-mouse IgG-HRP (Santa Cruz Sc-2005) for 2 h at RT. The slides were then washed with TBST and incubated with the liquid DAB+ substrate solution of the chromogen system (DAKO) until a brown color was observed. After staining, the tissue was counter-stained with hematoxylin for 30 sec and rinsed under

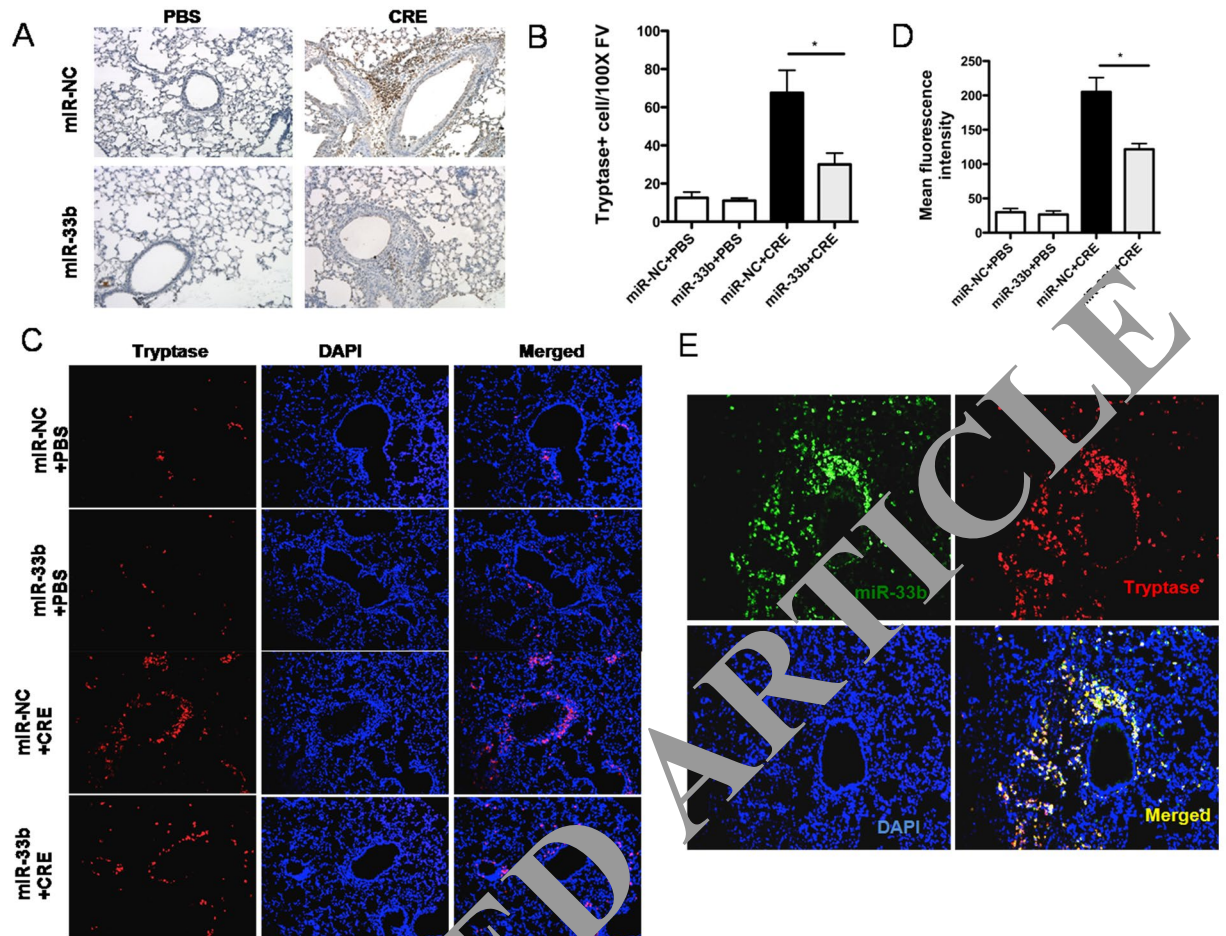


Figure 3. MiR-33b inhibits mast cell expression in asthma. (A–C) Representative images of DAB-stained tryptase and immunofluorescence in lung tissue sections of PBS- ($n = 3$) or CRE-challenged C57BL/6 mice that were transfected with miR-NC and miR-33b. (B–D) Quantitative data of DAB staining and immunofluorescence. (E) Representative images of co-immunofluorescence staining with tryptase and GFP-miR-33b in the lung tissues of CRE-challenged WT mice. The quantitative data are representative of 3 independent experiments. The data are means \pm SEM. * $P < 0.05$.

...ing water for 10 min. The slides were then dipped in 100% alcohol three times and then xylene three times. Finally, photographs were taken with a Nikon microscope.

Immunofluorescence. The lung sections were blocked with a serum-free protein-blocking solution (Dako, Glostrup, Denmark) and incubated with the primary antibodies overnight at 4 °C. After the sections were washed with TBST and incubated with fluorescent dye-conjugated secondary antibodies at room temperature for 1 h, nuclear staining was carried out with 6-diamidino-2-phenylindole, dihydrochloride (DAPI) (Thermo Fisher). Tryptase (ab2378, Abcam) and GFP (Cell Signaling Technology, cat# 2956) antibodies were used. Alexa Fluor-conjugated secondary antibodies (Invitrogen) were used to visualize the staining. Images were captured using a Nikon microscope. The intensity of co-staining was determined using image acquisition and analysis software (ImageJ) and presented as the mean fluorescence intensity per square micron.

Bone marrow-derived mast cell (BMMCs) cultures. BMMCs were obtained by culturing mouse bone marrow cells as described previously²². The BMMCs were generated from C57BL/6 mice and cultured at a starting density of 20×10^5 cells/ml at 37 °C in a humidified atmosphere containing 5% CO₂ in RPMI-1640 medium, 2 mM GlutaMAX™, 0.1 mM non-essential amino acids, 1 mM sodium pyruvate, 100 µg/ml streptomycin, 100 U/ml penicillin, 10% heat inactivated FBS (Invitrogen), 10 mM HEPES, 50 µM β-2-mercaptoethanol (2-ME), and 30% WEHI-3-conditioned medium as a source of IL-3 for 4–6 weeks. The mast cell phenotype was examined by flow cytometric analysis using Abs specific for c-Kit (2B8; eBioscience) and FcεRI (MAR-1; eBioscience).

Degranulation assays. The BMMCs were harvested and sensitized with 1 µg/ml anti-OVA IgE (E-C1, ChondrexInc) in microplates. The plates were incubated overnight at 37 °C with miR-33b or miR-NC transfection for 24 h and then washed with Tyrode's buffer. Triplicate cultures of BMMCs were incubated in a 96-well plate for another 30 min at 37 °C with 10 µg/ml OVA (1×10^5 cells/well). The reaction was stopped by placing the

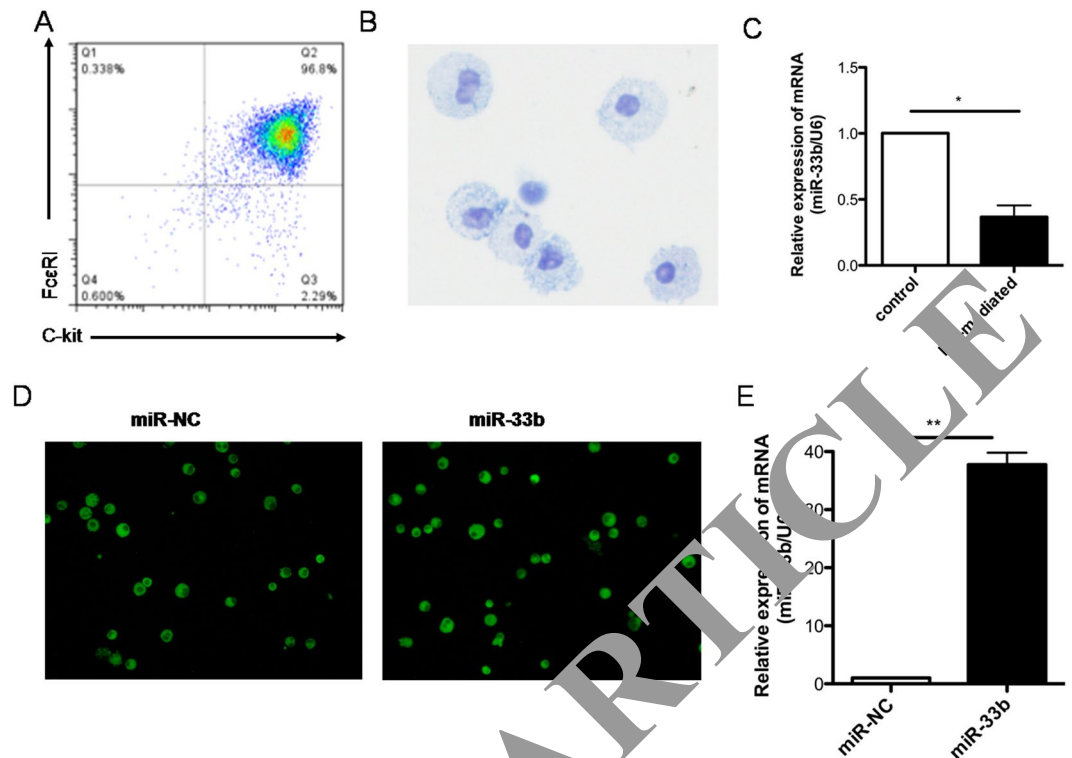


Figure 4. MiR-33b was down-regulated in IgE-mediated activation of bone marrow mast cells (BMMCs) and was overexpressed in transfected BMMCs. (A) Representative FACS for c-Kit and FcεRI expression in BMMCs. (B) Toluidine blue was used to identify the mast cells. (C) The expression of miR-33b was analyzed using qRT-PCR in BMMCs that were activated through IgE. (D,E) Immunofluorescence and qRT-PCR were used to evaluate the miR-33b transfection efficiency.

plate on ice for 5 min, and 10 μ l aliquots of the supernatants were collected for β -hexosaminidase assay. Lysates of un-stimulated cells prepared in Tyrode's buffer containing 0.5% TritonX-100 were used to obtain the total β -hexosaminidase content. Degranulation was expressed as a percentage of total β -hexosaminidase activity in the input cells.

LTC₄ assays and IL-13 test. LTC₄ was measured in 1×10^5 anti-OVA IgE-sensitized mast cells following stimulation with OVA (10 μ g/ml OVA). The supernatants were collected after 30 min of challenge, and LTC₄ was measured with an enzyme-linked immunosorbent assay kit according to the manufacturer's instructions (Cayman Chemical). However, for the IL-13 test, the supernatants were collected after 6 h of OVA challenge and were analyzed using ELISA. The coating and detection Abs specific for IL-13 were from eBiosciences.

Intradermal cutaneous anaphylaxis. A total of 10^6 BMMCs that had been transfected with miR-33b or miR-NC were injected intradermally (i.d.) into the paws of C57BL/6 mice. Four weeks after reconstitution, the transferred mast cells were sensitized by injecting 200 ng of E-C1 in 20 μ l PBS, and the left paw was injected with 20 μ l PBS as a negative control. After 24 h, OVA was administered intravenously together with Evans blue dye, and 30 min later, the mice were sacrificed by terminal anesthesia. Tissue sections were taken from the areas around the intradermal injection sites. The sectioned tissues were then weighed and treated with formamide at 55 $^{\circ}$ C for 24 h. The absorbance was measured at 620 nm. The data are expressed as Evan's blue in ng/mg tissue.

Intracellular calcium measurement. IgE-sensitized BMMCs were loaded with 2.5 μ M Fluo-4-AM (Molecular Probes) for 1 h in the dark at room temperature. After washing with CIB, the cells were challenged with 10 μ g/ml OVA and imaged at 488 nm excitation to detect the intracellular free calcium continuously for 90–120 sec. Each experiment was performed at least three times, and at least 100 cells were analyzed each time.

Statistical analysis. The data are presented as the mean \pm SEM with $n = 8$ animals per group. The significance of differences between two groups was determined by one-way ANOVA (nonparametric test) using Prism software. When 2 groups were compared, an unpaired 2-tailed Student's t-test was used. Statistical significance was reported if $P < 0.05$ was achieved.

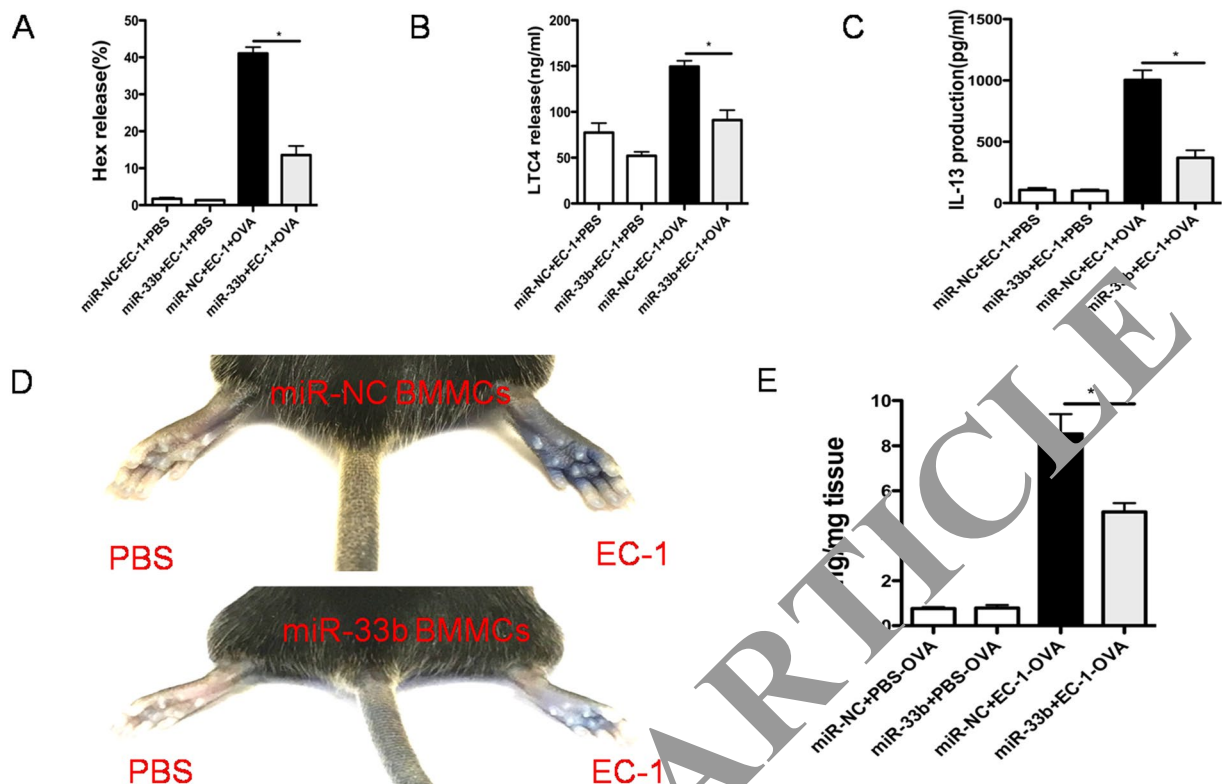


Figure 5. MiR-33b significantly decreased mast cell degranulation and PCA reactions. (A) BMMCs from C57BL/6 mice were sensitized with $1 \mu\text{g/ml}$ OVA and IgE (E-C1) for 24 h and then stimulated with $10 \mu\text{g/ml}$ OVA for 30 min. Degranulation was monitored as the release of β -hexosaminidase. (B,C) miR-33b decreased the IgE-mediated LTC4 and IL-13 production. (D) Representative images of Evans blue-stained extravasation into the paws 30 min after intravenous injection of OVA in C57BL/6 mice treated with miR-NC BMMCs or miR-33b BMMCs ($n = 6$ each group). (E) Quantification of the extravasation of Evans blue leakage into the paws. The absorbance was measured at 620 nm, and the data are expressed as Evan's blue in ng/mg tissue. The data are presented as the mean \pm SEM. Comparisons between miR-NC BMMC- and miR-33b BMMC-transfected C57BL/6 mice were performed using two-tailed Student's t-test. * $P < 0.05$.

Results

Expression of lentiviral miR-33b in the asthmatic mice.

To investigate the role of miR-33b in lung inflammation, mice were sensitized on days 0 to 4 with an intra-tracheal instillation of $400 \mu\text{g/ml}$ CRE. Non-sensitized control animals received the same volumes of PBS alone. Five days after the first sensitization, the mice were challenged by an intra-tracheal instillation with the same concentration of CRE once only on days 10 to 14. We found that miR-33b expression was highly decreased in the CRE-challenged group compared to the PBS group (Fig. 1A). Next, we constructed an asthma model following intranasal infection with the LV miR-33b (Fig. 1B). Notably, after the mice were treated with LV miR-33b, miR-33b was significantly up-regulated, indicating that the LV-host gene transduction was successfully accomplished in these mice (Fig. 1C). In addition, LV miR-33b and miR-NC were labeled with GFP, and GFP staining further confirmed that miR-33 had successfully reached the lungs (Fig. 1D).

MiR-33b regulates eosinophil influx and lung inflammation in response to CRE.

To better understand the role of miR-33b in asthma, we performed a histological analysis. This analysis demonstrated that miR-33 decreased the inflammatory cell infiltration and the associated goblet cell hyperplasia as assessed by HE and PAS staining (Fig. 2A,B). Bronchoalveolar lavage fluid (BALF) was harvested at 24 h after the last challenge, and the total cell and differential inflammatory cell counts were performed. The CRE-challenged miR-NC mice showed increasing numbers of total cells and eosinophils in the BALF. However, we found a significant reduction in total cells and eosinophil recruitment in the BALF of the CRE-challenged miR-33b mice (Fig. 2C). The AHR to methacholine was decreased in the CRE-challenged miR-33b mice compared to the CRE-challenged miR-NC mice (Fig. 2D). The serum levels of IgE and IgG1 were also significantly lower in the CRE-challenged miR-33b mice (Fig. 2E). Furthermore, Th2 cytokines including IL-4, IL-5 and IL-13 in the BALF were also reduced in the CRE-challenged miR-33b mice (Fig. 2F), which indicated systemic protection from the adaptive Th2 response in the CRE-challenged miR-33b mice.

MiR-33b inhibited mast cell expression in asthma.

There is compelling evidence that mast cells play a key role in the pathophysiology and pathogenesis of asthma, but the potential for mast cell activation to be

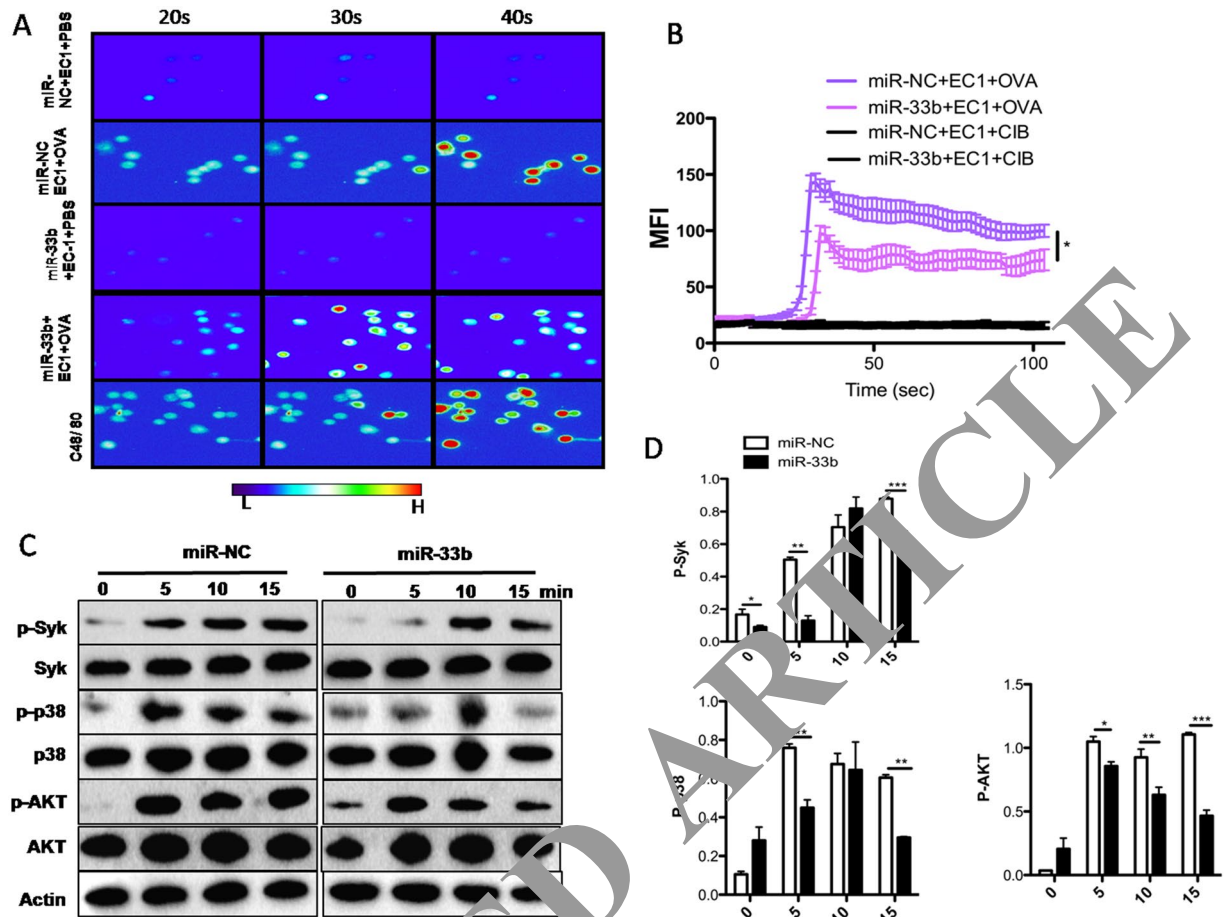


Figure 6. MiR-33b signaling events associated with mast cell function. (A) Representative Fluo-4 fluorescence heat map images of anti-OVA IgE-sensitized BMMCs showing the changes in $[Ca^{2+}]_i$ that were induced by OVA ($n = 3$). (B) Representative imaging traces. Each colored line represents the average of the traces for each treatment. CIB: Ca^{2+} imaging buffer. (C,D) Representative immunoblot of IgE-initiated early and late signaling events in the miR-NC or miR-33b transfected BMMCs. The quantitative data are representative of 3 independent experiments. The data are the means \pm SEM. * $P < 0.05$. ** $P < 0.01$.

affected by miR-33b has not been explored. To examine the role of mast cells in our model, we quantified the number of mast cells in the lung tissues of the CRE-exposed mice. The majority of mast cells were located near the epithelial surfaces, especially in the skin and airways. The increase in tryptase staining in lung sections from CRE-challenged mice was greatly reduced in mice transfected with miR-33b (Fig. 3A–D). The release of tryptase potentially damage and activate the bronchial epithelium as well as contribute to airway wall remodeling. Furthermore, as shown in Fig. 3E by GFP⁺Tryptase⁺ staining, the CRE-challenged miR-33b mice exhibited miR-33b expression in mast cells. These findings show that mast cells respond to CRE challenge and suggest that miR-33b may regulate mast cell migration and activation.

MiR-33b was down-regulated following IgE-mediated activation of BMMCs and was over-expressed in transfected BMMCs. BMMCs were generated from wild-type mice by culturing for 4–6 weeks ($c-kit^+FceRI^+$; Fig. 4A,B). To examine the effects of miR-33b on IgE-activated BMMCs, miR-33b expression in control and IgE-treated BMMCs was analyzed. The results showed that miR-33b expression was significantly lower in the IgE-treated group than in the control group (Fig. 4C). To assess the role of miR-33b on the IgE-mediated activation of BMMCs, we transfected GFP-miR-33b or GFP-miR-NC into the BMMCs using Lipofectamine 2000 reagent. After 72 h of transfection, we photographed the immunofluorescence to evaluate the success of the transfection (Fig. 4D). miR-33b expression was strongly increased in BMMCs that had been transfected with miR-33b (Fig. 4E).

MiR-33b significantly decreased the mast cell degranulation and PCA reactions. Although miR-33b was down-regulated in IgE-treated BMMCs, the role of miR-33b in regulating mast cell function was still elusive. To determine whether miR-33b contributes to the activation of mast cells, mast cell degranulation [β -hexosaminidase (Hex)] and several mediators (e.g., histamine, LTC₄, and cytokine IL-13) were detected and analyzed in the mast cells from C57BL/6 mice. BMMCs were sensitized with an OVA-specific IgE antibody (EC1)

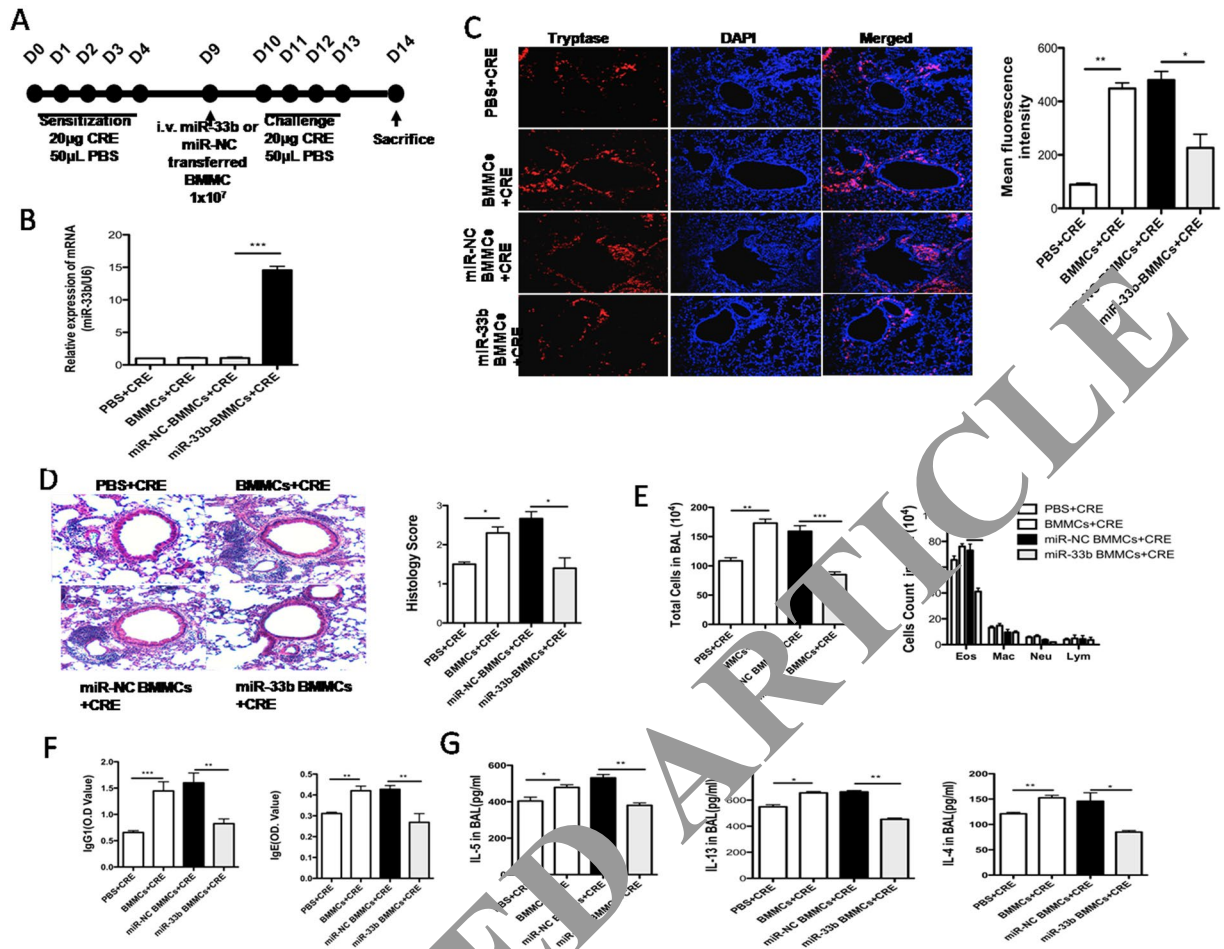


Figure 7. MiR-33b inhibits lung inflammation in mice engrafted with miR-33b BMMCs. **(A)** Protocol for the adoptive transfer of BMMCs in the cockroach allergen-induced mouse model of asthma. **(B)** qRT-PCR was used to measure miR-33b expression. **(C)** Tryptase expression and quantities in the lung sections of CRE-challenged C57BL/6 mice with adoptively transferred miR-NC or miR-33b BMMCs. **(D)** Representative H&E-stained paraffin lung tissue sections from C57BL/6 ($n = 6$) that were adoptively transferred with miR-NC or miR-33b BMMCs in the CRE-induced mouse model of asthma. **(E)** Cellular inflammation as indicated by the total cell number and differentiated leukocyte cell numbers in the BALF. **(F)** The specific IgE and IgG1 levels of the transferred mice were determined using ELISA assays. **(G)** The Th2 cytokines IL-4, -5 and -13 were measured in the transferred mice model. The data are representative of three independent experiments ($n = 4-6$ mice/group). The data are presented as the means \pm SEM. * $P < 0.05$, ** $P < 0.01$, *** $P < 0.001$.

for 24 h, followed by cross-linking of the surface-bound IgE with antigen for 30 min. The results showed that the levels of degranulation were significantly suppressed in the mast cells that had been transfected with miR-33b compared with those treated with miR-NC (Fig. 5A). Moreover, decreases in LTC₄ secretion (Fig. 5B) and interleukin 13 (IL-13) expression (Fig. 5C) were also observed in the miR-33b-treated BMMCs. *In vivo*, we used a passive cutaneous anaphylaxis (PCA) model to further test the ability of miR-33b to inhibit mast cell activation. A total of 10⁶ BMMCs that had been transfected with miR-33b or miR-NC were intra-dermally (i.d.) injected into the paws of C57BL/6 mice. Four weeks after reconstitution, the transferred mast cells were sensitized with 200 ng E-C1 in 20 μ l PBS or 20 μ l PBS as a negative control for 48 h, and an immediate-type allergic reaction was induced by the intravenous injection of OVA and Evans blue dye. An anaphylactic response was determined by the extravasation of Evans blue dye, indicative of vascular leakage²². Compared to PBS, a significant enhancement of PCA was noted in the OVA-sensitized and challenged mice (Fig. 5D,E). However, the PCA reaction was suppressed in the mice that had been intra-dermally treated with the miR-33b-transfected BMMCs.

MiR-33b signaling events associated with mast cell function. The elevation of intracellular calcium concentration ($[Ca^{2+}]_i$) is one of the critical common signaling events in the activation of mast cell degranulation²³. As shown in Fig. 6A,B, both the immediate and sustained increases in $[Ca^{2+}]_i$ in response to OVA challenge were reduced in BMMCs that had been transfected with miR-33b. Furthermore, in association with the increased levels of $[Ca^{2+}]_i$, changes in several of the signals upstream and downstream of IgE binding were

noted in the miR-33b-transfected BMMCs upon stimulation with IgE and OVA antigen. Notably, the miR-33b-transfected BMMCs showed decreased levels of p-p38, p-AKT, and p-syk (Fig. 6C,D).

MiR-33b BMMCs reduce CRE-induced lung inflammation. To directly demonstrate a role of miR-33b in lung inflammation, CRE-challenged C57BL/6 mice were intravenously administered BMMCs that had been transfected with miR-NC or miR-33b before the CRE challenge (Fig. 7A). The control groups included administration of PBS or naïve BMMCs. To provide further evidence that the miR-33b level affected the mast cell transfer model, we collected lung tissue to examine miR-33b expression. The data demonstrated that the level of miR-33b was increased in the CRE model after engraftment with miR-33b BMMCs, as shown in Fig. 7B. Next, we assessed the efficiency of mast cell recruitment in the C57BL/6 mice in the adoptive transfer experiment by analyzing the number of Tryptase⁺ cells in the lung tissues of these tested mice (Fig. 7C). Specifically, we found that the C57BL/6 mice into which the miR-NC BMMCs had been adoptively transferred exhibited increased numbers of mast cells (Fig. 7C). The mice engrafted with the miR-NC BMMCs developed significantly more severe lung inflammation than those engrafted with the miR-33b BMMCs. Histological examination revealed that transfer of the miR-33b BMMCs decreased inflammatory cell infiltration (Fig. 7D). The disease severity paralleled the inflammatory cell numbers and the cytokines that were observed in these mice. The mice reconstituted with miR-33b BMMCs demonstrated significantly fewer eosinophils and produced significantly less IL-4, IL-5, IL-13, IgE, and IgG1 compared with those engrafted with miR-NC BMMCs (Fig. 7E–G). These observations indicate that miR-33b in mast cells may inhibit CRE-induced allergic inflammation and asthma *in vivo*.

Discussion

In this study, we demonstrated for the first time a role of miR-33b in the development of allergic inflammation using the CRE-induced allergic asthmatic murine model. A regulatory role of miR-33b in mediating mast cell function was previously unknown and had not been reported. We also uncovered a novel critical regulatory role of miR-33b in the inhibition of CRE-induced asthma by suppressing mast cell function.

Deregulated T_H2 cell responses cause allergies and asthma. Over the past few decades, several studies have demonstrated the importance of a positive feedback loop that involves the hallmark T_H2 cell-associated cytokine IL-4 and the transcription factor STAT6^{24,25}. In addition to IL-4, T_H2 cells also express the cytokines IL-5 and IL-13, which drive type 2 inflammation through their effect on myeloid cells²⁶. In recent years, many studies have shown that miRNAs are associated with the development of asthma. However, the miRNA-mediated regulation of T_H2 cell differentiation is poorly understood. A previous study found that miR-18a, miR-126, let-7e, miR-155, and miR-224 were down-regulated while miR-498, miR-187, miR-874, miR-143, and miR-886-3p were up-regulated in asthmatic patients compared to controls²⁷. In the asthmatic mouse model, miR-21, miR-145 and miR-106a are up-regulated in ovalbumin (OVA)- or house dust mite (HDM)-challenged mice^{28–31}. In addition, approximately 50% of miR-155-deficient mice develop lung inflammation in which some hallmarks of type 2 inflammation associated with asthma are elevated⁹.

MiR-33b is located in introns of the sterol regulatory element-binding protein (SREBP)-encoding genes that control cholesterol and lipid homeostasis in concert with their host gene products³². It has been reported that miR-33 augments macrophage lipid rafts and enhances proinflammatory cytokine induction and NF-κB activation by LPS³³. The relationship between miR-33b and asthma is unknown. We therefore sought to determine whether miR-33b plays a critical role in airway inflammation and Th2 cell-associated cytokines in the CRE-induced asthma model. The results showed that several key elements of asthma, including the infiltration of inflammatory cells, especially eosinophils, Th2 cytokines in the BALF, AHR, and specific IgE production were reduced in the CRE-treated miR-33b^{33,34}, which indicated that the Th2 response plays an important role in the miR-33b-mediated inhibition of asthma development.

Mast cells are found in the skin and in all mucosal tissues under homeostatic conditions and are located below the epithelium in connective tissue surrounding blood cells, smooth muscle, mucous, and hair follicles. In the respiratory tract, the immune response to mast cell activation results in airway constriction, increased mucous production, and cough³⁵. Mast cells play a central role in immediate allergic reactions and inflammation. They are able to release potent inflammatory mediators, such as proteases, histamine, and cytokines to recruit inflammatory cells³⁶. Several studies have reported that miRNA can regulate mast cell function^{11–14}. For example, miR-221, which was overexpressed in an asthma model, increased IL-4 secretion in mast cells by regulating PTEN, p38, and NF-κB expression³⁷. MiR-223 promotes degranulation via the PI3K/Akt pathway by targeting IGF-1R in mast cells³⁸. Recent publications have noted that the treatment of mice with anti-miR-33 oligonucleotides reduces the expression of proinflammatory genes (IL-1, TNFα, and iNOS) and increases the expression of an anti-inflammatory gene (IL-10) in atherosclerotic lesions^{39–41}. MiR-33 positively regulates the proinflammatory M1 programming of macrophages by LPS/TNFα⁴⁰. MiR-33 can augment macrophage lipid rafts and enhance proinflammatory cytokine induction and NF-κB activation by LPS³³. In our study, we focused on whether miR-33b modulates mast cell function. Interestingly, miR-33b significantly inhibited the IgE-mediated mast cell functions *in vitro* and *in vivo*. This result differed from the observations in macrophages, and the effects of this miR may depend upon the cell type and immunological context. Mast cells may have a key effect on tissue remodeling, especially in the context of AHR and mucus hyper-secretion, by releasing proteases such as tryptase³⁵. We showed that tryptase staining was much less obvious in miR-33b BMMCs that were treated with CRE. Furthermore, the PCA response and extent of mast cell degranulation, LTC4, and IL-13 were decreased in the miR-33b BMMCs. These results suggest that mast cell activation and mast cell-related allergic responses could be regulated by miR-33b. To further test whether miR-33b inhibited CRE-induced asthma through mast activation, we constructed a mast cell knock-in model. The mice into which miR-33b BMMCs were adoptively transferred showed a reduced airway inflammatory signal, which was consistent with the intranasal injection the mouse model.

Nevertheless, the extent and mechanisms by which miR-33b could regulate mast cells is unknown. FcεRI-dependent signaling pathways control mast cell degranulation. IgE/FcεRI induces activation of Lyn, which phosphorylates FcεRI ITAMs and activates Syk following ITAM binding. MAPK signaling and Ca²⁺ are also increased following Syk activation, and these processes regulate mast cell function^{42,43}. The influx of Ca²⁺ is the key factor that induces mast cell activation. The transient release of Ca²⁺ from the endoplasmic reticulum (ER) stores subsequently induces the prolonged influx of Ca²⁺ through store-operated calcium release-activated calcium (CRAC) channels in the plasma membrane. The influx of Ca²⁺ that is mediated by CRACM1 is essential for mast cell activation⁴⁴. Zhou reported that FICZ-treated mast cells showed enhanced levels of MAPK pathway proteins, especially the phosphorylation of ERK, which accompanies Ca²⁺ release²². The IgE-induced Ca²⁺ influx induces the production of ROS, which results in the prolongation of ERK phosphorylation to activate mast cell degranulation⁴⁵. It has been reported that miR-221 promotes IgE-mediated mast cell degranulation through the PI3K/Akt/PLCγ/Ca²⁺ signaling pathway⁴⁶. One study reported that the p-AKT and IGF1R levels increased following miR-223 down-regulation in mast cells. In addition, inhibition of PI3K and IGF1 resulted in the induction of IL-6 secretion in miR-223-expressing mast cells, which indicated that miR-223 reduces IL-6 secretion in mast cells by inhibiting the IGF1R/PI3K signaling pathway⁴⁷. Furthermore, our data suggested that miR-33b regulates mast cell function through Ca²⁺ influx and MAPK signaling. The PI3K/Akt pathway is essential for cell growth, metabolism, survival, and inflammation. In the present study, it was also found that miR-33b suppressed mast cell degranulation by regulating Akt expression.

In conclusion, using a CRE-induced model of allergic asthma in mice, we demonstrated a critical role of miR-33b in inhibiting lung inflammation. We demonstrated here that the activation of miR-33b associated with mast cell function restrains the signaling that is induced through IgE/FcεRI binding. Our findings identified a new fundamental node of the cross-talk between miR-33b and mast cells and may suggest new effects and potential applications of the therapeutic targeting of miR-33 in asthma.

References

- Willart, M. A. & L. B. The danger within: endogenous danger signaling in asthma. *Clin. Exp. Allergy* **39**, 12–19 (2009).
- Paul, W. E. & Z. J. How are T(H)2-type immune responses initiated and amplified? *Nat Rev Immunol* **10**, 225–235 (2010).
- Sjöberg, L. C. Interleukin-33 exacerbates allergic bronchoconstriction in the mice via activation of mast cells. *Allergy* **70**, 514–521 (2015).
- Oczyppok, E. A. *et al.* Pulmonary receptor for advanced glycation end-products promotes asthma pathogenesis through IL-33 and accumulation of group 2 innate lymphoid cells. *J Allergy Clin Immunol* **136**, 747–756 (2015).
- Eggleston, P. A., Rosenstreich, D., Lynn, H. *et al.* Relationship of indoor allergen exposure to skin test sensitivity in inner-city children with asthma. *The Journal of allergy and clinical immunology* **102**, 563–570 (1998).
- Galli, S. J., Grimaldeston, M. & Tsai, M. Immunoregulatory mast cells: negative, as well as positive, regulators of immunity. *Nat Rev Immunol* **8**, 478–486 (2008).
- Kalesnikoff, J. & Galli, S. New developments in mast cell biology. *Nat Immunol* **9**, 1215–1223 (2008).
- Bartel, D. P. MicroRNAs: genomic biogenesis, mechanism, and function. *Cell* **116**, 281–297 (2004).
- Rodriguez, A. *et al.* Requirement of miR-155 for normal immune function. *Science* **316**, 608–611 (2007).
- Polikepahad, S. *et al.* Proinflammatory role for let-7 MicroRNAs in Experimental Asthma. *J Biol Chem* **285**, 30139–30149 (2010).
- Mayoral, R. J. *et al.* MicroRNA-221-222 regulate the Cell Cycle in Mast Cells. *J Immunol* **182**, 433–445 (2009).
- Mayoral, R. J. *et al.* miR-221 influences Effector Functions and Actin Cytoskeleton in Mast Cells. *Plos One* **6**, doi:ARTN e26133 (2011).
- Ishizaki, T. *et al.* miR126 positively regulates mast cell proliferation and cytokine production through suppressing Spred1. *Genes Cells* **16**, 803–814 (2011).
- Molnar, V. *et al.* MicroRNA-132 targets HB-EGF upon IgE-mediated activation in murine and human mast cells. *Cell Mol Life Sci* **69**, 793–808 (2012).
- Rise, S. *et al.* Delta5 desaturase mRNA levels are increased by simvastatin via SREBP-1 at early stages, not via PPARalpha, in THP-1 cells. *Lipids* **42**, 97–105 (2007).
- Cheng, Y. *et al.* Transforming growth factor-beta-induced miR143 expression in regulation of non-small cell lung cancer cell viability and invasion capacity *in vitro* and *in vivo*. *Int J Oncol* **45**, 1977–1988 (2014).
- Qu, J. J. *et al.* microRNA-33b inhibits lung adenocarcinoma cell growth, invasion, and epithelial-mesenchymal transition by suppressing Wnt/β-catenin/ZEB1 signaling. *Int J Oncol* **47**, 2141–2152 (2015).
- Qu, J. J. *et al.* miR-33b inhibits tumor EMT and migration in lung squamous cell carcinoma by targeting TWIST1. *Int J Clin Exp Pathol* **9**, 789–801 (2016).
- Yin, H. X. *et al.* DNA Methylation mediated down-regulating of MicroRNA-33b and its role in gastric cancer. *Sci Rep* **6** (2016).
- Takwi, A. A. L. *et al.* A statin-regulated microRNA represses human c-Myc expression and function. *Embo Molecular Medicine* **4**, 896–909 (2012).
- Kyung, S. L. *et al.* Inhibition of phosphoinositide 3-kinase attenuates allergic airway inflammation and hyperresponsiveness in murine asthma model. *FASEB J* **20**, 455–465 (2006).
- Zhou, Y. *et al.* Aryl hydrocarbon receptor controls murine mast cell homeostasis. *Blood* **121**, 3195–3204 (2013).
- Gilfillan, A. M. & Tkaczyk, C. Integrated signalling pathways for mast-cell activation. *Nat Rev Immunol* **6**, 218–230 (2006).
- Locksley, R. M. Asthma and allergic inflammation. *Cell* **140**, 777–783 (2010).
- Paul, W. E. & Zhu, J. How are T(H)2-type immune responses initiated and amplified? *Nat Rev Immunol* **10**, 225–235 (2010).
- Ansel, K. M., Djuretic, I., Tanasa, B. & Rao, A. Regulation of Th2 differentiation and Il4 locus accessibility. *Annu. Rev. Immunol* **24**, 607–656 (2006).
- Suojalehto, H. *et al.* Altered MicroRNA Expression of Nasal Mucosa in Long-Term Asthma and Allergic Rhinitis. *Int Arch Allergy Imm* **163**, 168–178 (2014).
- Lu, T. X., Munitz, A. & Rothenberg, M. E. MicroRNA-21 is up-regulated in allergic airway inflammation and regulates IL-12p35 expression. *J Immunol* **182**, 4994–5002 (2009).
- Mattes, J., Collison, A., Plank, M., Phipps, S. & Foster, P. S. Antagonism of microRNA-126 suppresses the effector function of TH2 cells and the development of allergic airways disease. *Proc Natl Acad Sci USA* **106**, 18704–18709 (2009).
- Collison, A., Mattes, J., Plank, M. & Foster, P. S. Inhibition of house dust mite-induced allergic airways disease by antagonism of microRNA-145 is comparable to glucocorticoid treatment. *J Allergy Clin Immunol* **128**, 160–167 (2011).
- Sharma, A. *et al.* Antagonism of mmu-mir-106a attenuates asthma features in allergic murine model. *J Appl Physiol (1985)* **113**, 459–464 (2012).

32. Lai, L. *et al.* MicroRNA-33 Regulates the Innate Immune Response via ATP Binding Cassette Transporter-mediated Remodeling of Membrane Microdomains. *J Biol Chem* **291**, 19651–19660 (2016).
33. Finkelman, F. D. & Urban, J. F. Jr. The other side of the coin: the protective role of the TH2 cytokines. *J Allergy Clin Immunol* **107**, 772–780 (2001).
34. Lambrecht, B. N. & Hammad, H. The airway epithelium in asthma. *Nat Med* **18**, 684–692 (2012).
35. Amin, K. *et al.* Inflammation and structural changes in the airways of patients with atopic and nonatopic asthma. BHR Group. *Am J Respir Crit Care Med* **162**, 2295–2301 (2000).
36. Borish, L. & Joseph, B. Z. Inflammation and the allergic response. *Med Clin North Am* **76**, 765–787 (1992).
37. Zhou, Y. *et al.* miRNA-221-3p Enhances the Secretion of Interleukin-4 in Mast Cells through the Phosphatase and Tensin Homolog/p38/Nuclear Factor-kappaB Pathway. *PLoS One* **11** (2016).
38. Wang, Q. *et al.* Down-regulation of microRNA-223 promotes degranulation via the PI3K/Akt pathway by targeting IGF-1R in mast cells. *PLoS One* **10** (2015).
39. Distel, E. *et al.* miR33 inhibition overcomes deleterious effects of diabetes mellitus on atherosclerosis plaque regression in mice. *Circ Res* **115**, 759–769 (2014).
40. Ouimet, M. *et al.* MicroRNA-33-dependent regulation of macrophage metabolism directs immune cell polarization in atherosclerosis. *J Clin Invest* **125**, 4334–4348 (2015).
41. Rayner, K. J. *et al.* Antagonism of miR-33 in mice promotes reverse cholesterol transport and regression of atherosclerosis. *J Clin Invest* **121**, 2921–2931 (2011).
42. Kraft, S. & Kinet, J. P. New developments in FcεpsilonRI regulation, function and inhibition. *Nat Rev Immunol* **7**, 365–378 (2007).
43. Shumilina, E. *et al.* Blunted IgE-mediated activation of mast cells in mice lacking the CD2+-activated calcium channel KCa3.1. *J Immunol* **180**, 8040–8047 (2008).
44. Vig, M. *et al.* Defective mast cell effector functions in mice lacking the CRACM1 pore subunit of store-operated calcium release-activated calcium channels. *Nat Immunol* **9**, 89–96 (2008).
45. Sly, L. M. *et al.* IgE-induced mast cell survival requires the prolonged generation of reactive oxygen species. *J Immunol* **181**, 3850–3860 (2008).
46. Xu, H., Gu, L. N., Yang, Q. Y., Zhao, D. Y. & Liu, F. MiR-221 promotes IgE-mediated activation of mast cells degranulation by PI3K/Akt/PLCγ/Ca(2+) pathway. *J Bioenerg Biomembr* **48**, 293–299 (2016).
47. Yang, Q. *et al.* MicroRNA-223 affects IL-6 secretion in mast cells via the IGF1R/PI3K signaling pathway. *Int J Mol Med* **38**, 507–512 (2016).

Acknowledgements

This study was supported in part by grants from the National Key Scientific & Technology Support Program: Collaborative Innovation of Clinical Research for Chronic Obstructive Pulmonary Disease and Lung Cancer (No. 2013BAI09B09).

Author Contributions

L.J.M. and R.C.N. performed the experiments and wrote the manuscript; X.P.X. edited the references; B.L., Y.Q.L. and Y.Z. analyzed the data; and L.J.M. and R.C.N. modified the manuscript.

Additional Information

Competing Interests: The authors declare that they have no competing interests.

Publisher's note: Springer Nature remains neutral with regard to jurisdictional claims in published maps and institutional affiliations.



Open Access This article is licensed under a Creative Commons Attribution 4.0 International License, which permits use, sharing, adaptation, distribution and reproduction in any medium or format, as long as you give appropriate credit to the original author(s) and the source, provide a link to the Creative Commons license, and indicate if changes were made. The images or other third party material in this article are included in the article's Creative Commons license, unless indicated otherwise in a credit line to the material. If material is not included in the article's Creative Commons license and your intended use is not permitted by statutory regulation or exceeds the permitted use, you will need to obtain permission directly from the copyright holder. To view a copy of this license, visit <http://creativecommons.org/licenses/by/4.0/>.

© The Author(s) 2017